

Cooperative Effects

Seeded Supramolecular Polymerization in a Three-Domain Self-Assembly of an N-Annulated Perylenetetracarboxamide

Elisa E. Greciano and Luis Sánchez*^[a]

Abstract: The three-domain cooperative supramolecular polymerization of **1**, together with the lag time in which the monomeric species remains inactive, allows seeded supramolecular polymerization to be performed. The kinetic experiments demonstrate that only seeds based on the intermediate aggregate are able to propagate the supramolec-

ular polymerization of **1** from their active sites. The results presented herein constitute a new example of kinetically controlled supramolecular systems and contribute to expanding knowledge about the structural requirements of a self-assembling molecule to experience seeded supramolecular polymerization.

Introduction

In good correlation with the general polymerization strategy of a repetitive sequence of monomeric units to generate the polymeric chain, Lehn and co-workers reported the first example of a supramolecular polymer formed by hydrogen-bonding interactions between uracil and 2,6-diaminopyridines derivatives.^[1] From this first example, to date, great advances have been achieved in the area of supramolecular polymerization both from basic and practical points of view.^[2] The function of a supramolecular polymer is directly related to the mechanism followed by the monomeric units to form the polymeric chain. Thus, two extreme supramolecular polymerization mechanisms, isodesmic or nucleation–elongation, have been described and amply investigated.^[3] However, to emulate natural or man-made polymerization processes, such as actin polymerization or seeded living polymerization, respectively,^[4,5] far-from-equilibrium systems have been recently reported.^[6] The possibility of attaining kinetically controlled supramolecular polymers, together with the similarity of initiation–propagation in living polymerization and nucleation–elongation in a cooperative supramolecular polymerization, have inspired very few reports on the new concept of supramolecular polymerization known as living supramolecular polymerization (LSP), which yields supramolecular polymers with controlled length and narrow polydispersity.^[7]

LSP consists of cooperative supramolecular polymerization in which the spontaneous self-assembly of monomeric units, joined together by intramolecular noncovalent forces, is strongly accelerated by the addition of an initiator unable to

form the corresponding supramolecular polymers by itself. The coassembly of both monomers generates an active dimer that grows rapidly to form a supramolecular polymer.^[7] The spontaneous polymerization of a bowl-shaped corannulene derivative containing five amide groups exemplify the concept of LSP.^[8] Closely related with this idea are examples in which temporally inactive species can evolve to yield supramolecular polymerization in different ways: 1) by following two different elongation pathways in equilibrium (EQ) that provide aggregated systems with different properties (helicity or light absorption), or 2) by ensuring supramolecular polymerization is inactive until a specific seed is added. Competing pathways in the self-assembly of *S*-chiral oligo(*p*-phenylenevinylene), which yields the two opposite helical structures;^[6] the temporal evolution of *J* aggregates formed by porphyrin-based self-assembling molecules;^[9] and different emissive aggregated states generated in the self-assembly of a platinum(II) complex^[10] exemplify the first strategy. In the second strategy, for kinetically trapped species to evolve, the monomeric species can be kinetically trapped in an inactive state by the presence of an additional noncovalent interaction that generates an aggregation-incompetent conformation. The addition of a seed initiates rapid supramolecular polymerization. This is the case for the accelerated self-assembly of a series of perylene bisimide (PDI) organogelators.^[11]

The abovementioned examples share three common features that allow valuable information to be extracted to define the requisites for a kinetically trapped self-assembling system to yield accelerated supramolecular polymerization: 1) aggregation proceeds through a cooperative mechanism; 2) the nucleation regimen is retarded, which allows kinetic control of the process; and 3) it is possible to prepare the seeds in a separate manner that can be further act as initiators. In addition, from a chemical structure point of view, a number of the reported examples of seeded supramolecular polymerization (SSP) also share the presence of a 3,4,5-trialkoxy-*N*-(alkoxy)benzamide moiety capable of forming different supramolecular

[a] E. E. Greciano, Prof. Dr. L. Sánchez
Departamento de Química Orgánica I Facultad de Ciencias Químicas
Universidad Complutense de Madrid
Ciudad Universitaria s/n; 28040 Madrid (Spain)
E-mail: lusamar@quim.ucm.es

Supporting information for this article can be found under <http://dx.doi.org/10.1002/chem.201602344>.

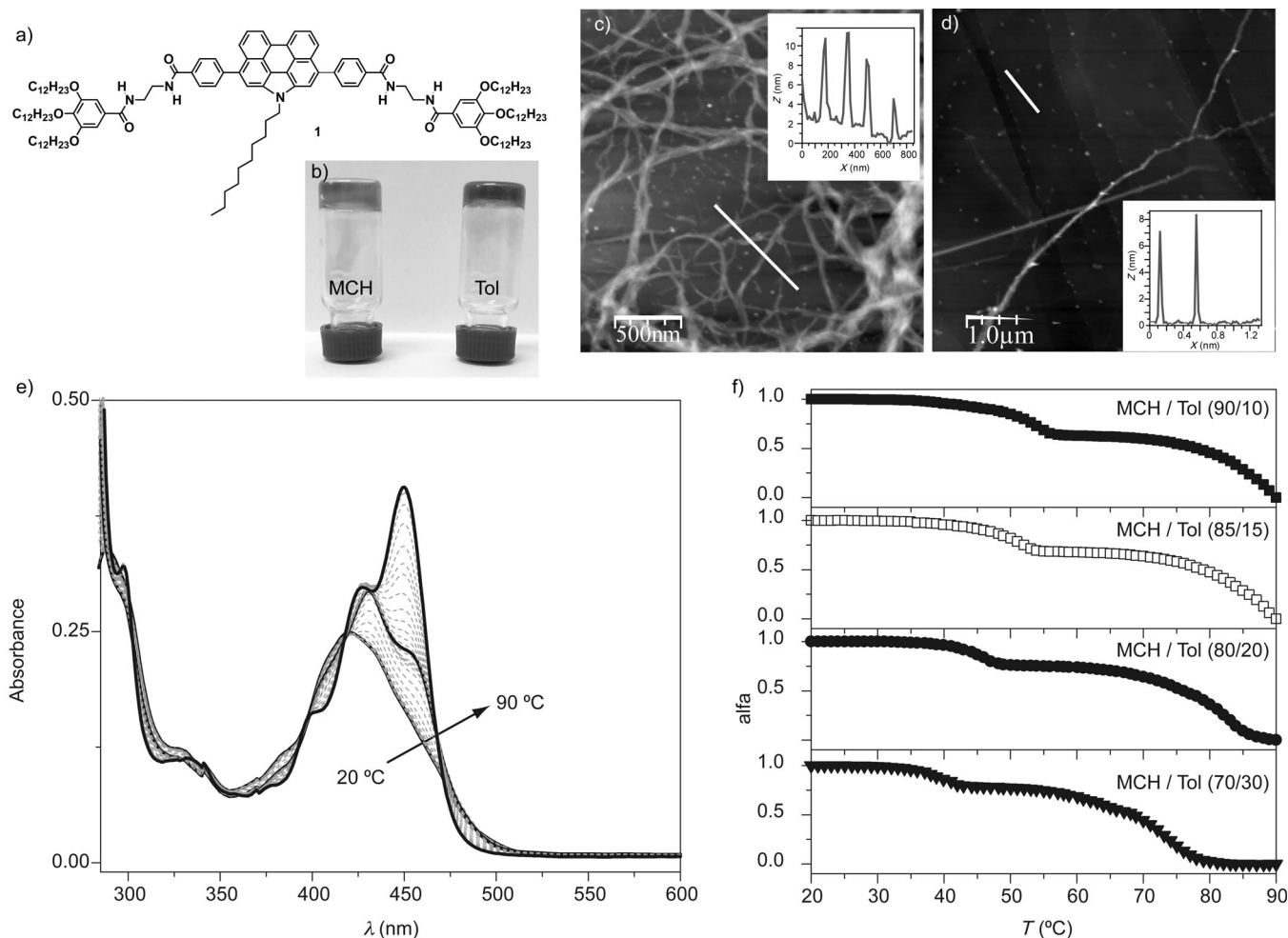


Figure 1. a) Chemical structure of the N-annulated perylene-3,4,9,10-tetracarboxamide **1**. b) Photograph of the organogels formed by **1** in methylcyclohexane (MCH) and toluene (Tol). AFM height images of **1** on highly oriented pyrolytic graphite (HOPG) as a substrate in MCH (c) and Tol (d) as solvents (298 K, 1×10^{-5} M; z scale = 35 (c) and 25 nm (d)). The insets in c) and d) show the height profiles along the white lines. e) Temperature-dependent UV/Vis spectra of **1** in MCH/Tol 70/30 (1×10^{-5} M, from 363 to 293 K). The black lines depict the UV/Vis spectra of **1** at 20, 52, and 90 °C. f) Plot of the variation of the degree of aggregation of **1** versus temperature at $c_T = 1 \times 10^{-5}$ M and in different mixtures of MCH/Tol.

structures through the formation of intra- or intermolecular hydrogen-bonding interactions.^[9,11]

To increase our knowledge on the structural rules that a relatively simple self-assembling unit should fulfil to experience an efficient SSP process, herein we report on the seeded self-assembly of an N-annulated perylene endowed with two amide functional groups in each of its peripheral side chains (**1**; Figure 1 a). Similarly to the PDIs and porphyrins that have been reported to experience a seeded process, compound **1** is decorated with a 3,4,5-trialkoxy-N-(alkoxy)benzamide moiety; supramolecular polymerization in Tol is cooperative with a thermal hysteresis. These features make it possible to kinetically trap the monomeric species. Interestingly, the addition of a more apolar solvent, such as MCH, provokes a unique three-step cooperative supramolecular polymerization process. We have detected three different species by UV/Vis: the monomeric unit (M), an intermediate aggregated species (I), and the completely aggregated state (A). We have evaluated SSP experienced by **1** at different concentrations and upon adding different seeds, corresponding to I and A. In the former case, acceleration of

supramolecular polymerization, which is diagnostic of SSP, is higher than that in the latter case. The results presented herein expand our comprehension of the mechanistic and structural details of supramolecular polymers to provide a general route to advanced, functional, aggregated structures.

Results and discussion

Synthesis and supramolecular polymerization mechanism

Compound **1** was obtained in a similar multistep protocol to that previously reported by our research group to prepare N-annulated perylenedicarboxamides (see Scheme S1 in the Supporting Information).^[12] NMR and FTIR spectroscopic data, as well as the corresponding high-resolution mass spectra, confirm the proposed chemical structure (see the Supporting Information).

A first indication of the tendency of **1** to self-assemble in solution through hydrogen-bonding interactions between the amides and π stacking of the aromatic unit is inferred by pre-

liminary concentration-dependent ^1H NMR spectroscopy experiments in CDCl_3 . In good correlation with some other examples,^[13] increasing the concentration results in a downfield shift of both resonances at $\delta \approx 7.6$ and 7.4 ppm, corresponding to the inner and outer amides, respectively, and in a shielding effect on the protons corresponding to the aromatic core, especially those at $\delta \approx 8.6$ ppm, which are ascribable to protons of the bay position of the perylene unit (Figure S1 in the Supporting Information). This trend of **1** to self-assemble in more apolar solvents, such as MCH and Tol, has been also studied by dynamic light scattering (DLS). The correlation functions obtained for **1** in MCH exhibit a sum of exponential decays together with an oscillatory term. This behavior has been previously described for highly absorbing macromolecules or aggregated species and it has been rationalized by the presence of different species in convective motion.^[14] The average hydrodynamic radii obtained by analyzing the correlation functions obtained for **1** in MCH is 296 nm (Figure S2a in the Supporting Information). However, CONTIN analysis of the correlation functions of **1** in Tol shows a very broad distribution of particle sizes indicative of the presence of species with very different morphologies (Figure S2b in the Supporting Information).

Compound **1** readily form gels in apolar solvents, such as MCH or Tol, which implies the formation of organized supramolecular structures (Figure 1 b). The solvent strongly conditions the morphology of the aggregates visualized by AFM of dilute solutions of **1** (1×10^{-5} M). In more apolar MCH, bundles of fibers constitutive of the organogel are clearly visible. The diameter of the thinner fibers is around 7 nm (Figure 1 c and Figure S3 in the Supporting Information). However, the AFM images of **1** in Tol reveal the formation of nanoparticles together with isolated fibrillar structures (Figure 1 d). The dissimilar morphologies observed in MCH or Tol have also been reported for PDI organogelators capable of undergoing SSP.^[11b]

Variable-temperature UV/Vis (VT-UV/Vis) experiments, in different solvent at different concentrations, have been utilized to achieve a detailed investigation of the supramolecular polymerization mechanism. In analogy with that reported for the aggregated state of a comparable N-annulated perylenedicarboxamide,^[12a] compound **1** in an aggregated state features a broad band centered at $\lambda = 423$ nm that splits upon heating into three bands at $\lambda = 398$, 427, and 452 nm (Figure 1 e). The strong trend of **1** to self-assemble in an apolar solvent such as MCH and at a total concentration (c_T) as low as 5×10^{-6} M impedes the observation of the abovementioned spectroscopic features of **1** in a molecularly dissolved state. Consequently, the addition of a more polar cosolvent, such as Tol, is necessary to obtain the molecularly dissolved state for **1**. The corresponding cooling curves of **1** in mixtures of MCH/Tol show nonsigmoidal curves with very high elongation temperatures (T_e), that is, the temperature at which the nucleation regimen changes to the elongation one,^[3] which is indicative of cooperative supramolecular polymerization. Closer inspection of the cooling curves shows a subtle transition at intermediate temperatures (Figure S4 in the Supporting Information). The transition between the nucleation and elongation regimens cannot be observed because of the strong trend of **1** to aggregate.

However, a clear intermediate transition is observed at around 50 °C in the heating curves. Interestingly, increasing the percentage of Tol allows two defined transitions at around 80 and 50 °C to be unambiguously observed; these are diagnostic of a three-step supramolecular polymerization (Figure 1 f and Figure S5 in the Supporting Information). The heating curves of **1** involve the contribution of three different species, namely, the monomeric unit M; annealed, aggregated intermediate species I; and completely aggregated state A. The UV/Vis spectra at 20, 52, and 90 °C show different crossing points that are indicative of the formation of three different chemical species (Figure 1 f). Notably, the elongation temperatures observed in the heating (T_e) and cooling (T_e') processes, even if very high, are not identical; thus indicating thermal hysteresis. This behavior has been identified in comparable PDIs as a fingerprint of a kinetically controlled supramolecular polymerization in which an inactive monomeric species is present.^[11]

The T_e and T_e' values decrease notably with Tol as the solvent in the corresponding heating and cooling curves (Figure 2 a). The increasing difference between these two transition temperatures indicates that the supramolecular polymerization of **1** can be kinetically controlled in this solvent. The VT-UV/Vis experiments performed in Tol show that the spectrum at 20 °C exhibits the same shape as that observed for **1** at intermediate temperatures (≈ 50 °C) in mixtures of MCH/Tol (Figure 2 b). These studies suggest that in the aggregation process of **1** in Tol only the denaturation and annealing steps occur involving the monomeric unit M and the annealed, aggregated intermediate species I.

The nonsigmoidal transitions observed for the denaturation–annealing processes in both Tol and mixtures of MCH/Tol can be fitted to the EQ model to extract the corresponding thermodynamic parameters of the self-assembly process, namely, the enthalpy of elongation, ΔH_e ; the entropy of elongation, ΔS ; and the nucleation penalty, ΔH_n (Table 1 and Figure S6 in the Supporting Information).^[15] Considering the differences in polarity of the solvent and concentration of the sample, the values of the thermodynamic parameters are similar.

Data extracted from the VT-UV/Vis experiments of **1** show good agreement with that reported for the kinetically controlled supramolecular polymerization of PDIs^[11] with a striking difference in the three-step aggregation process. The formation of up to nine-membered pseudocycles through intramolecular hydrogen-bonding interactions between bis-amides or bis-ureas has been utilized to justify the origin of the inactivation of the monomers in the case of PDIs.^[16] Thus, the formation of an intramolecular hydrogen-bonding interaction between the N–H of the amide functional group and one of the

Table 1. Thermodynamic parameters of the supramolecular polymerization of **1** derived from the EQ model.

	Tol (1×10^{-4} M)	MCH/Tol (70/30; 1×10^{-5} M)
ΔH_e [kJ mol ⁻¹]	-109.7 ± 3.5	-103.1 ± 3.1
ΔS [J K ⁻¹ mol ⁻¹]	-258 ± 11	-198 ± 9
ΔH_n [kJ mol ⁻¹]	-15.1 ± 0.8	-18.0 ± 0.9

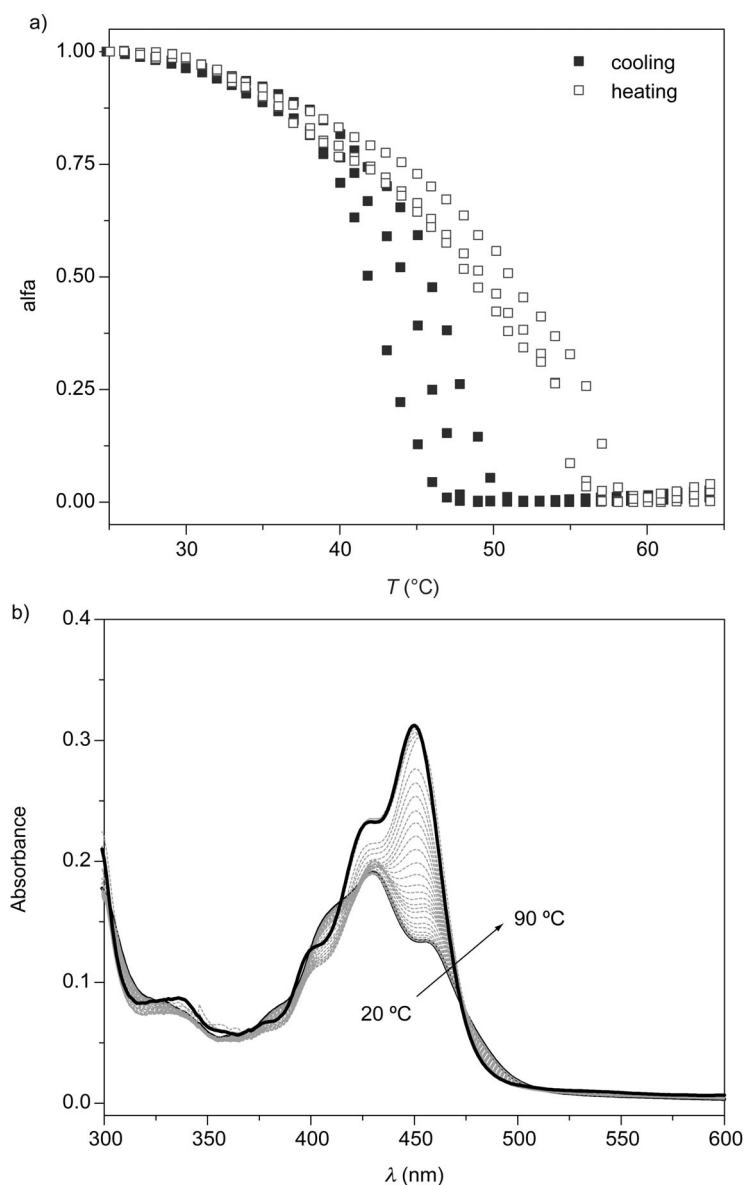


Figure 2. a) Heating (\square) and cooling (\blacksquare) curves of **1** at different concentrations in Tol ($c_T = 1.5 \times 10^{-4}$, 1.0×10^{-4} , and 0.9×10^{-4} M). b) VT-UV/Vis spectra of **1** in Tol (1×10^{-4} M).

carbonyls of the imide moiety produces a seven-membered pseudocycle that cannot elongate to form the supramolecular polymer. However, compound **1** is endowed with two amide functional groups attached to an ethylene spacer. The structural features of **1** are appropriate to form two different seven-membered pseudocycles involving the two amide groups (Figure 3a). The synergy of UV/Vis, variable-temperature (VT) ^1H NMR, and 2D-ROESY spectroscopy experiments in chloroform at $c_T = 2 \times 10^{-3}$ M has been utilized to demonstrate the formation of the inactivated monomer of **1**.^[17] Under these conditions of concentration and solvent, the UV/Vis spectrum of **1** exhibits the characteristic pattern of the monomeric species M with three absorption maxima at $\lambda = 398$, 427, and 452 nm (Figure S7a in the Supporting Information).

The VT- ^1H NMR spectra of **1** at 2×10^{-3} M show a slight shielding effect on both triplets corresponding to the amide

protons upon increasing the temperature (Figure S7b in the Supporting Information). The shift of both resonances can be reasonably assigned to the intramolecular hydrogen-bonding interaction between the N–H of the inner amide and the carbonyl of the outer amide and also to the intramolecular hydrogen-bonding interaction between the N–H of the outer amide and the carbonyl of the inner amide (Figure 3a). Definitive evidence of the formation of the seven-membered pseudocycles involving the two amide groups has been obtained by a 2D-ROESY experiment (Figure 3b). This experiment shows through-space intramolecular contacts between the *ortho* proton of the benzamide unit with the N–H of the outer amide, with the proton of the external 3,4,5-trialkoxybenzamide moiety, and also with the methylene joint to the oxygen in this same unit (arrows in Figure 3a and circles in Figure 3b). These through-space contacts can only be explained by the formation of intramolecular hydrogen-bonded rings.

Notably, these kinetically inactivated monomeric rings still have additional N–H and carbonyl groups that, under the appropriate conditions of concentration and/or temperature, can readily grow up to form a supramolecular polymer (Figure 3c). These intermediate species, I, in which the four amides participate in two intramolecular and two intermolecular hydrogen-bonding interactions, feature the UV/Vis spectrum observed at temperatures of around 50 °C in mixtures of MCH/Tol and the spectrum at room temperature in pure Tol with an absorption maximum at $\lambda = 430$ nm and two shoulders at $\lambda = 410$ and 456 nm (Figures 1c and 2b). The rearrangement of the two intramolecular hydrogen bonds into intermolecular hydrogen bonds induces stretching of the ethylene spacer, which allows the formation of a hydrogen-bonding array between the four amides and optimizes π stacking of the N-annulated perylene (Figure 3c).^[18] As a consequence, the UV/Vis spectrum of the completely aggregated species A of **1**, observed at low temperatures in mixtures of MCH/Tol, exhibits a broad absorption maximum at $\lambda = 423$ nm (Figure 1c). This spectrum coincides exactly with that previously reported by our research group for the aggregated species of an N-annulated perylenedicarboxamide organogelator.^[12a] The conversion of the kinetically inactivated monomers M into the intermediate supramolecular polymers I, and the further conversion of these intermediate aggregates into the final supramolecular polymer A can reasonably justify the three-step supramolecular polymerization process observed in the corresponding heating curves of **1** in mixtures of MCH/Tol.

Time-dependent SSP

The cooperative supramolecular polymerization of **1**, the hysteresis loop observed in the T_e and T_e' values, and the possibility of forming inactivated monomeric species imply the possibility

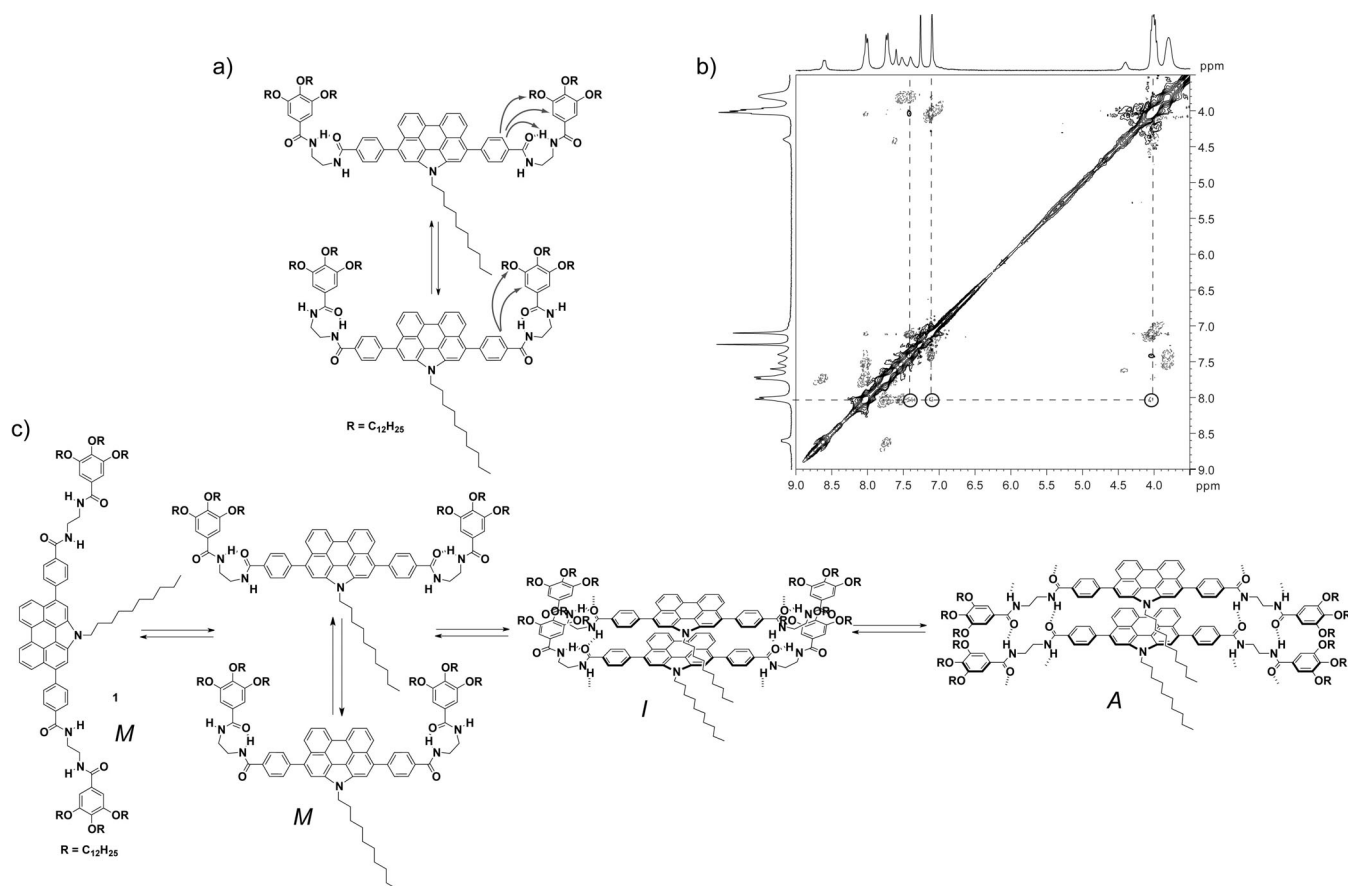


Figure 3. a) Chemical structure of the inactivated monomeric species of **1** showing the two possible intramolecular hydrogen-bonded rings. b) 2D-ROESY NMR spectrum (CDCl₃, 300 MHz, 8 mm, 298 K) of **1**. The circles highlight the intermolecular through-space coupling signals between the protons of the hydrogen-bonded rings indicated by the curved arrows in a). c) Schematic representation of the proposed three-step equilibria that yield the supramolecular polymerization of **1**.

of far-from-EQ processes and, consequently, the possibility of investigating the operation of SSP. The difference between the T_e and T_e' values, which increase with decreasing c_T , facilitates an effective temperature range to maintain inactivated monomeric species of **1** (Figure S8 in the Supporting Information). In this range of temperatures, the formation of the kinetically trapped monomeric species is preferred over supramolecular polymerization. However, the thermodynamically more stable supramolecular polymers of **1** should induce the transformation of monomeric hydrogen-bonded rings **M** into intermediate **I** or completely aggregated **A** over time. The spectroscopic differences found between the **M**, **I**, and **A** species can be utilized for identification to follow the kinetic evolution of the supramolecular polymerization of **1** by monitoring different parameters, such as concentration or temperature (Figure 4a and b). All time-dependent experiments were performed through the rapid heating of a sample to 90 °C, followed by fast cooling (25 K min⁻¹) to the corresponding temperature. The time-dependent experiment was launched 1 min after reaching this temperature. Due to the very high values of T_e found in the mixtures of MCH/Tol, we performed the time-dependent experiments by using Tol as the solvent.

We first evaluated the effect of concentration on the kinetic evolution of the supramolecular polymerization of **1**. At a rela-

tively high concentration (4×10^{-5} M), the kinetic profile shows two transitions. The first one can be ascribed to the very rapid conversion of the kinetically trapped monomers into the intermediate aggregates **I** (Figure 4a). The second transition yields the completely aggregated species **A**, as demonstrated by the absorption spectrum, which exhibits a broad band centered at $\lambda = 423$ nm (Figure S9a in the Supporting Information). Upon decreasing the concentration to 1×10^{-5} M, the kinetic profile shows a single transition with a clear sigmoidal shape that is diagnostic of an autocatalytic process in which the nucleation and elongation regimens are involved, but separated by a lag time of around 10 min (Figure 4a).^[8,11] At this concentration, the UV/Vis spectrum of the final species corresponds to the intermediate aggregate **I** with an absorption maximum at $\lambda = 430$ nm and two shoulders at $\lambda = 410$ and 456 nm (Figure S9b in the Supporting Information). These kinetic experiments demonstrate that, upon increasing the concentration of **1** in Tol, it is possible to reach the completely aggregated species with four intermolecular hydrogen bonds between the amides, which were only observed previously in mixtures of MCH/Tol.

Considering the hysteresis loop observed between the T_e and T_e' values, we also evaluated the kinetic evolution of the transformation of the monomeric species by changing the

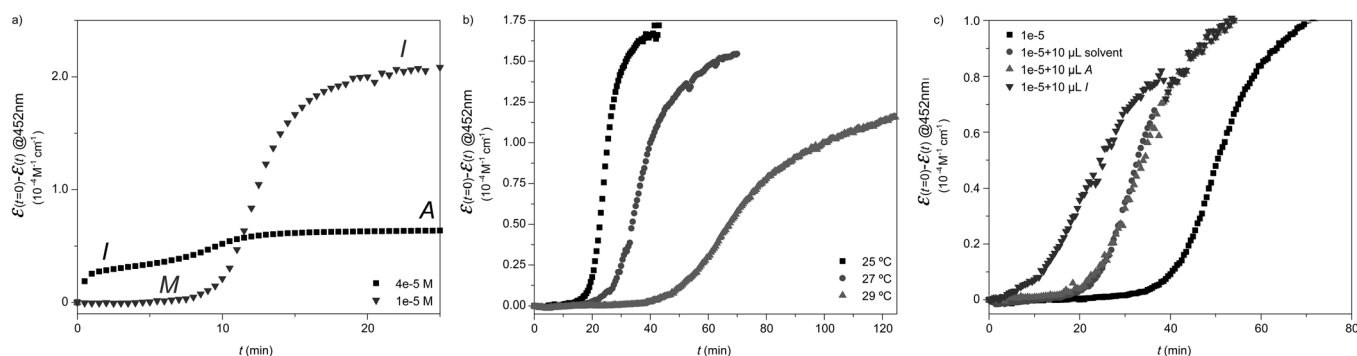


Figure 4. Kinetic profiles of aggregate formation in Tol a) at different concentrations ($25\text{ }^{\circ}\text{C}$, $4 \times 10^{-5}\text{ M}$ and $1 \times 10^{-5}\text{ M}$), and b) at different temperatures at a concentration of $1 \times 10^{-5}\text{ M}$. c) Kinetic profiles of the SSP of **1** by adding different seeding species at $29\text{ }^{\circ}\text{C}$.

temperature. Increasing the temperature results in kinetically retarded nucleation, in which the intramolecularly hydrogen-bonded monomeric rings are trapped longer; up to 40 min at $29\text{ }^{\circ}\text{C}$ (Figure 4b). In all cases, the sigmoidal shape of the kinetic profiles indicates an autocatalytic nucleation–elongation process that can be utilized to perform SSP. Unlike the previous examples of SSP,^[8,11] compound **1** can form two different aggregates (I and A) with perfectly defined spectroscopic features. Therefore, we have prepared two different seeds to initiate acceleration of the supramolecular polymerization of **1**. Following a similar strategy to that described for PDIs,^[11] we prepared both seeds of I and A species by sonicating a $1 \times 10^{-5}\text{ M}$ solution of **1** in MCH/Tol (70/30) for different time intervals, and following the absorption spectra as a fingerprint of the nature of the seed.

Taking into account the experimental data extracted from the time-dependent supramolecular polymerization experiments, seeded polymerization was performed at a concentration of $1 \times 10^{-5}\text{ M}$ in Tol at $29\text{ }^{\circ}\text{C}$ (Figure 4c). We first evaluated the ability of the seed corresponding to the intermediate aggregate to accelerate the supramolecular polymerization of **1**. Thus, the addition of the seed ($10\text{ }\mu\text{L}$) prepared by sonicating a $1 \times 10^{-5}\text{ M}$ solution of **1** in a mixture of MCH/Tol (70:30) for 10 min (Figure S10 in the Supporting Information), to achieve partially aggregated species I, into a freshly prepared monomeric solution of **1** ($1 \times 10^{-5}\text{ M}$ in Tol, heated to $90\text{ }^{\circ}\text{C}$ and rapidly cooled to $29\text{ }^{\circ}\text{C}$) reduced the lag time from 40 to 10 min (Figure 4c). This lag time is reduced or totally cancelled out by adding increasing amounts of the seeding sample (Figure S10 in the Supporting Information). The acceleration of the supramolecular polymerization of **1** has also been evaluated by adding the same amount ($10\text{ }\mu\text{L}$) of the mixture of MCH/Tol (70:30). In this case, the lag time is slightly reduced from 40 to 20 min, which implies that the supramolecular polymers of **1** can be propagated from the active sites of the intermediate aggregated seed. Finally, we also evaluated the capability of the seed corresponding to the fully aggregated species A of **1**, obtained by sonicating a $1 \times 10^{-5}\text{ M}$ solution of **1** in a mixture of MCH/Tol (70:30) for only 1 min, to accelerate the supramolecular polymerization of **1** (Figure S11 in the Supporting Information). In this case, after the addition of this seed of A species ($10\text{ }\mu\text{L}$), the lag time of the kinetic process is exactly the

same as that achieved for the addition of the mixture MCH/Tol (70:30; $10\text{ }\mu\text{L}$; Figure 4c). These data indicate that completely aggregated A species does not possess active sites to propagate the supramolecular polymerization of **1**, which, under these conditions, is only accelerated by the presence of the less polar solvent MCH.

Conclusion

The supramolecular polymerization of N-annulated perylene-tetracarboxamide **1** has been thoroughly investigated by using different conditions of concentration and solvent. The studies presented herein contribute to increasing knowledge of the structural requirements necessary for a self-assembling unit to experience far-from-EQ aggregation. Compound **1**, which readily forms organogels in apolar solvents, self-assembles cooperatively into fibrillar supramolecular structures in MCH or into nanoparticles together with isolated fibrillar structures in Tol. This cooperative supramolecular polymerization of **1** is strongly conditioned by the solvent and heating/cooling cycles. Thus, a three-step supramolecular polymerization process is observed for **1** in a mixture of MCH/Tol, which indicates the formation of two different aggregated species, I and A, that show perfectly distinguishable absorption features. VT-UV/Vis experiments in Tol show that the cooperative supramolecular polymerization of **1** yields the partially aggregated species I and also a hysteresis loop in the elongation temperatures. This hysteresis loop allows kinetic studies to be developed to control the supramolecular polymerization of **1** through the inactivation of the monomeric species. UV/Vis, VT- ^1H NMR, and 2D-ROESY experiments at $c_T = 2 \times 10^{-3}\text{ M}$ in chloroform have been utilized to demonstrate the formation of intramolecular hydrogen bonds between the amide functional groups to generate the inactivated monomer species of **1**. Time-dependent experiments demonstrate the evolution of these monomeric species into aggregates. At relatively high concentrations ($4 \times 10^{-5}\text{ M}$), the kinetic profile shows the rapid conversion of monomeric species into fully aggregated supramolecular structures. At a lower concentration ($1 \times 10^{-5}\text{ M}$), the monomeric species remains inactive for a time ranging from 10 to 40 min, depending on the temperature, yielding intermediate aggregates I. This lag time has been harnessed to perform SSP by using dif-

ferent seeds. The kinetic experiments demonstrate that only seeds based on intermediate aggregate I are able to propagate the supramolecular polymerization of **1** from the active sites. The results presented herein expand our knowledge of the structural requirements necessary for a self-assembling molecule to experience LSP to enhance and/or modulate the physical, chemical and/or optical properties of the final supramolecular structures. Work is currently in progress in our research group to further elucidate both experimentally and theoretically the nature of the inactivated monomeric species, as well as on three-step supramolecular polymerization involving three different monomeric, partially aggregated, and completely aggregated species.

Acknowledgements

This work was supported by the MINECO of Spain (CTQ2014-53046-P), and the Comunidad de Madrid (NanoBIOSOMA, S2013/MIT-2807). E.E.G. thanks the Universidad Complutense de Madrid for a predoctoral grant.

Keywords: cooperative effects · kinetics · polymers · self-assembly · supramolecular chemistry

- [1] C. Fouquey, J.-M. Lehn, A.-M. Levelut, *Adv. Mater.* **1990**, *2*, 254–257.
- [2] a) T. Aida, E. W. Meijer, S. I. Stupp, *Science* **2012**, *335*, 813–817; b) L. Brunsveld, B. J. B. Folmer, E. W. Meijer, R. P. Sijbesma, *Chem. Rev.* **2001**, *101*, 4071–4097; c) S. S. Babu, V. K. Praveen, A. Ajayaghosh, *Chem. Rev.* **2014**, *114*, 1973–2129; d) C. Kulkarni, S. Balasubramanian, S. J. George, *ChemPhysChem* **2013**, *14*, 661–673; e) C. Rest, R. Kandaneli, G. Fernández, *Chem. Soc. Rev.* **2015**, *44*, 2543–2572.
- [3] a) T. F. A. De Greef, M. M. J. Smulders, M. Wolffs, A. P. H. J. Schenning, R. P. Sijbesma, E. W. Meijer, *Chem. Rev.* **2009**, *109*, 5687–5754; b) F. Aparicio, F. García, L. Sánchez, *Encyclopedia of Polymer Science and Technology* (Ed. M. Peterca), Wiley, Hoboken, **2012**, pp. 549–578.
- [4] a) M. Kasai, S. Asakura, F. Oosawa, *Biochim. Biophys. Acta* **1962**, *57*, 22–31; b) S. Asakura, G. Eguchi, T. Iino, *J. Mol. Biol.* **1964**, *10*, 42–56.
- [5] a) X. Wang, G. Guerin, H. Wang, Y. Wang, I. Manners, M. A. Winnik, *Science* **2007**, *317*, 644–647; b) J. B. Gilroy, T. Gädt, G. R. Whittell, L. Chabanne, J. M. Mitchels, R. M. Richardson, M. A. Winnik, I. Manners, *Nat. Chem.* **2010**, *2*, 566–570.
- [6] a) P. A. Korevaar, S. J. George, A. J. Markvoort, M. M. J.; Smulders, P. A. J.; Hilbers, A. P. H. J. Schenning, T. F. A. De Greef, E. W. Meijer, *Nature* **2012**, *481*, 492–496; Smulders, P. A. J.; Hilbers, A. P. H. J. Schenning, T. F. A. De Greef, E. W. Meijer, *Nature* **2012**, *481*, 492–496; b) F. Aparicio, B. Nieto-Ortega, F. Nájera, F. J. Ramírez, J. T. López Navarrete, J. Casado, L. Sánchez, *Angew. Chem. Int. Ed.* **2014**, *53*, 1373–1377; *Angew. Chem.* **2014**, *126*, 1397–1401.
- [7] a) R. D. Mukhopadhyay, A. Ajayaghosh, *Science* **2015**, *349*, 241–242; b) R. Deng, X. Liu, *Nat. Chem.* **2015**, *7*, 472–473; c) D. van der Zwaag, T. F. A. de Greef, E. W. Meijer, *Angew. Chem. Int. Ed.* **2015**, *54*, 8334–8336; *Angew. Chem.* **2015**, *127*, 8452–8454; d) E. Mattia, S. Otto, *Nat. Nanotechnol.* **2015**, *10*, 111–119.
- [8] J. Kang, D. Miyajima, T. Mori, Y. Inoue, Y. Itoh, T. Aida, *Science* **2015**, *347*, 646–651.
- [9] a) S. Ogi, K. Sugiyasu, S. Manna, S. Samitsu, M. Takeuchi, *Nat. Chem.* **2014**, *6*, 188–195; b) S. Ogi, T. Fukui, M. L. Jue, M. Takeuchi, K. Sugiyasu, *Angew. Chem. Int. Ed.* **2014**, *53*, 14363–14367; *Angew. Chem.* **2014**, *126*, 14591–14595.
- [10] A. Aliprandi, M. Mauro, L. De Cola, *Nat. Chem.* **2016**, *8*, 10–15.
- [11] a) S. Ogi, V. Stepanenko, K. Sugiyasu, M. Takeuchi, F. Würthner, *J. Am. Chem. Soc.* **2015**, *137*, 3300–3307; b) S. Ogi, V. Stepanenko, J. Thein, F. Würthner, *J. Am. Chem. Soc.* **2016**, *138*, 670–678.
- [12] a) F. García, J. Buendía, S. Ghosh, A. Ajayaghosh, L. Sánchez, *Chem. Commun.* **2013**, *49*, 9278–9280; b) J. Buendía, E. E. Greciano, L. Sánchez, *J. Org. Chem.* **2015**, *80*, 12444–12452.
- [13] a) F. García, P. M. Viruela, E. Matesanz, E. Ortí, L. Sánchez, *Chem. Eur. J.* **2011**, *17*, 7755–7759; b) F. Aparicio, F. García, L. Sánchez, *Chem. Eur. J.* **2013**, *19*, 3239–3248.
- [14] A. Sehgal, T. A. P. Seery, *Macromolecules* **1999**, *32*, 7807–7814.
- [15] H. M. M. ten Eikelder, A. J. Markvoort, T. F. A. de Greef, P. A. J. Hilbers, *J. Phys. Chem. B* **2012**, *116*, 5291–5301.
- [16] a) S. H. Gellman, G. P. Dado, G.-B. Liang, B. R. Adams, *J. Am. Chem. Soc.* **1991**, *113*, 1164–1173; b) J. S. Nowick, M. Abdi, A. Bellamo, J. A. Love, E. J. Martinez, G. Noronha, E. M. Smith, J. W. Ziller, *J. Am. Chem. Soc.* **1995**, *117*, 89–99.
- [17] Compound **1** readily forms an organogel in Tol or deuterated Tol at $c_T = 0.5 \times 10^{-3}$ M; this impedes the detection of the inactivated monomer by ^1H NMR or UV/Vis spectroscopy.
- [18] F. Aparicio, E. Matesanz, L. Sánchez, *Chem. Eur. J.* **2014**, *20*, 14599–14603.

Received: May 17, 2016
Published online on ■■■■■, 0000

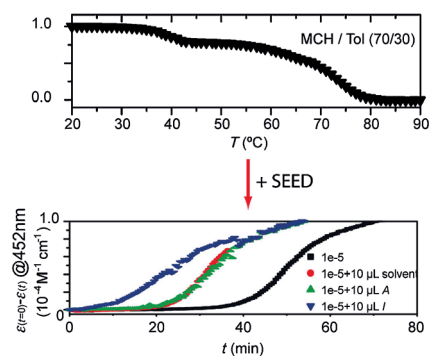
FULL PAPER

Cooperative Effects

*E. E. Greciano, L. Sánchez**



Seeded Supramolecular Polymerization in a Three-Domain Self-Assembly of an N-Annulated Perylenetetracarboxamide



Controlled coming together: The cooperative supramolecular polymerization of an N-annulated perylene endowed with two amide functional groups is investigated by changing the conditions of self-assembly. Control of the lag time in which the monomeric species remain inactive allows seeded supramolecular polymerization to be performed and studied with different seeding species (see figure).